World Journal of Radiology

Online Submissions: http://www.wjgnet.com/1949-8470office
wjr@wjgnet.com
doi:10.4329/wjr.v3.i12.298

World J Radiol 2011 December 28; 3(12): 298-305
ISSN 1949-8470 (online)

BRIEF ARTICLE

Image of tumor metastasis and inflammatory lymph node enlargement by contrast-enhanced ultrasonography

Takaya Aoki, Fuminori Moriyasu, Kei Yamamoto, Masafumi Shimizu, Masahiko Yamada, Yasuharu Imai

Takaya Aoki, Fuminori Moriyasu, Kei Yamamoto, Masafumi Shimizu, Masahiko Yamada, Yasuharu Imai, Department of Gastroenterology and Hepatology, Tokyo Medical University, 6-7-1, Nishishinjuku, Shinjyuku-ku, Tokyo 160-0023, Japan
Author contributions: All authors contribute equally to this article.
Correspondence to: Fuminori Moriyasu, MD, PhD, Department of Gastroenterology and Hepatology, Tokyo Medical University, 6-7-1 Nishi-Shinjuku Shinjukuku Tokyo 160-0023, Japan. moriyasu@tokyo-med.ac.jp
Telephone: +81-3-53256838 Fax: +81-3-53256840
Received: March 12, 2011 Revised: May 1, 2011
Accepted: July 4, 2011
Published online: December 28, 2011

Abstract

AIM: To compare the difference between tumor-induced lymph node enlargement and inflammation-induced lymph node enlargement by contrast-enhanced ultrasonography and pathological findings.

METHODS: A model of tumor-induced lymph node metastasis was prepared by embedding a VX2 tumor into the hind paws of white rabbits. A model of inflammation-induced enlargement was prepared by injecting a suspension of *Escherichia coli* into separate hind paws of white rabbits. Then, a solution of Sonazoid™ (GE Healthcare, Oslo, Norway) was injected subcutaneously in the proximity of the lesion followed by contrast-enhanced ultrasonography of the enlarged popliteal lymph nodes.

RESULTS: In the contrast-enhanced ultrasonography of the tumor-induced metastasis model, the sentinel lymph node was imaged. An area of filling defect was observed in that enlarged lymph node. In the histology examination, the area of filling defect corresponded to the metastatic lesion of the tumor. Contrast-enhanced ultrasonography of the model on inflammation-induced lymph node enlargement, and that of the acute inflammation model performed 3-7 d later, revealed dense staining that was comparatively uniform. The pathological findings showed acute lymphadenitis mainly due to infiltration of inflammatory cells. Contrast-enhanced ultrasonography that was performed 28 d post-infection in the acute inflammation model showed speckled staining. Inflammation-induced cell infiltration and fiberization, which are findings of chronic lymphadenitis, were seen in the pathological findings.

CONCLUSION: Sentinel lymph node imaging was made possible by subcutaneous injection of Sonazoid™. Contrast-enhanced ultrasonography was suggested to be useful in differentiating tumor-induced enlargement and inflammation-induced enlargement of lymph nodes.

Key words: Lymph node enlargement; Sentinel lymph node; Contrast-enhanced ultrasonography; Subcutaneous injection; Sonazoid™

Peer reviewer: Ragab Hani Donkol, Professor, Radiology Department, Aseer Central Hospital, 34 Abha, Saudi Arabia

Aoki T, Moriyasu F, Yamamoto K, Shimizu M, Yamada M, Imai Y. Image of tumor metastasis and inflammatory lymph node enlargement by contrast-enhanced ultrasonography. *World J Radiol* 2011; 3(12): 298-305 Available from: URL: http://www.wjgnet.com/1949-8470/full/v3/i12/298.htm DOI: http://dx.doi.org/10.4329/wjr.v3.i12.298

INTRODUCTION

Sonographic imaging eliminates the variations in scattered intensity that occur due to differences in acoustic impedance of various body tissue interfaces. Gaseous impedance is very small compared to impedance by body tissues that consists of liquids and solids. Thus, by using gaseous microbubbles, a strong contrast effect such as

an echo source can be achieved. This is the principle of contrast-enhanced ultrasonography and its development has made microvascular diagnosis possible.

When the acoustic pressure (amplitude) of the bombarding ultrasound wave is low, the microbubbles are comparatively stable, resonance occurs as scatter and reflector, and a non-linear signal is obtained. However, when the acoustic pressure of the bombarding ultrasonic wave is high, the microbubbles burst. With Sonazoid™, the threshold value of the resonating acoustic pressure when the MI value ranges from 0.2 to 0.4 is high compared to when SonoVue™ is used[1]. Sonazoid™ is a contrast agent that can be observed continuously with moderate acoustic pressure and without the microbubbles bursting.

The sentinel lymph node is a lymph node that cancer cells first reach if there is tumor metastasis to lymph nodes. The status of cancer cells reaching the subsequent lymph nodes that are downstream is judged based on the status of metastasis to this lymph node. It is also an important lymph node for decision making about the need for lymph node dissection. In various malignant tumors such as breast cancer, colon cancer and skin cancer, identification of the sentinel lymph node is now known to affect the choice of treatment[2-6].

Sentinel node navigation surgery (SNNS) is becoming the focus of attention as a lowly invasive form of treatment of early cancer. In SNNS, the site of the sentinel lymph node is different from that of the tumor. In addition, there are inter-individual variations, thus accurate identification of the sentinel lymph node is essential. To achieve this, substances that cause lymph node metastasis in the periphery of tumors are administered and the dynamics monitored to detect the direct inflow to the sentinel lymph node from the tumor lesion.

Radio-isotope (RI) procedures[4,7] and pigmentation techniques[8,9] are being used to identify sentinel lymph nodes such as those found in breast cancer and gastric cancer. The pigmentation techniques are inexpensive but need expertise. In addition, pigments can be administered during surgery of the lymphatic system where the rate of metastasis is high. The flow of lymph can be observed directly in real time. However, spreading of the pigment to distal lymph nodes is faster than to the sentinel lymph node, therefore, it is not necessarily the best procedure to identify the sentinel node. In addition, administration of pigments has been reported to cause anaphylaxis[10].

The RI procedure uses radioisotopes, therefore precision is high and quantitative identification is possible[11]. However, the equipment is massive and moreover, radioactive exposure of subjects and the examiner is a concern.

On the other hand, local injection of microbubble, which is a contrast agent, reveals the sentinel lymph node in ultrasonography[11-15]. Here, imaging performance in an animal model of malignant tumor-induced sentinel lymph node metastasis was investigated using the contrast agent Sonazoid™. In addition, a model of tumor-induced and a model of inflammation-induced swelling of lymph nodes were prepared to comparatively investigate the differences between tumor-induced enlargement and inflammation-induced enlargement of lymph nodes.

MATERIALS AND METHODS

Animal model

A total of 11 Japanese white rabbits (Clea Japan, Tokyo, Japan) weighing 2.5-3.5 kg (mean 2.9 kg) were used in the study. The rabbits were cared for by the Tokyo Medical University Animal Study Center staff and experimental protocols were approved by the Animal Ethical Committee of Tokyo Medical University.

The animals were kept in a room maintained in a day/night environment of alternate 12 h of light and darkness at a room temperature of 21℃.

Tumor-induced lymph node enlargement model

A model of VX2 tumor-induced metastatic lymph node enlargement was prepared in six animals. The VX2 tumor was embedded by injecting it into the femoral muscle of rabbit and from day 14 to 21, each muscle was excised. The isolated tumor was shredded and filtered under pressure using a commercial fine meshed filtering device while adding a small amount of physiological saline. After centrifugation at 700 r/min, the residue was suspended in physiological saline to make a cell concentration of about 2×10^6 cells/mL.

A total of 1 mL of that suspension was divided into several aliquots and each aliquot injected directly into the subcutaneous connective tissue of the hind paw of rabbit using an 18G injection needle. After 7-35 d had passed since the injection, VX2 tumors that had increased to 30-50 mm were found in the hind paws. The popliteal lymph nodes of these animals had enlarged from 12-18 mm and were used as the tumor-induced lymph node enlargement.

Coliform inflammation model

A coliform inflammation-induced lymph node enlargement model was prepared using five animals. Cultured colonies of coliform bacteria [*Escherichia coli* (*E. coli*), verotoxin non-producing] of 10 × 10 mm that had been collected from human clinical specimens were taken and dispersed in 10 mL physiological saline at 30℃ to prepare a coliform solution at a cell concentration of about 10^6 cells/mL.

For the inflammation-induced lymph node enlargement model, a total of 1 mL of this coliform solution was divided into several aliquots and each aliquot subcutaneously injected into the connective tissue of the hind paw of a white rabbit using an 18 gauge needle. From 3 to 28 d after the injection, tumors that had enlarged by 10 to 30 mm or connective tissue inflammation (cellulitis) were found in the hind paw. The popliteal lymph nodes of these rabbits had enlarged by 8 to 17 mm. The enlarged popliteal lymph nodes were confirmed with an ultrasound device and were used as the inflammation-

induced lymph node enlargement model.

Prior to observation, hair on the entire legs of the rabbits was shaved off and cleaned using commercial hair removing cream to make them hairless. This facilitated the observation by ultrasound.

The protocol of the study was performed in accordance with the specifications of the Ethics Committee on Animal Studies of Tokyo Medical University.

Ultrasound diagnostic device

The ultrasound device used was Aplio™XV (SSA-770A ultrasound diagnostic system Aplio™XV, Toshiba Medical Systems Co., Otawara, Japan) that was commercialized by Toshiba Medical Systems Corp for clinical use.

A 7.5 MHz linear type (PLT-704AT) probe was used. The contrast mode was Pulse Subtraction Imaging (PSI®), which is phase invasion harmonic. The acoustic pressure for the MI value was set at 0.2-0.4. The frame rate was set at 15 fps.

Dose of contrast and observations

The study was performed by intravenous injection under intravenous anesthesia. A 24G indwelling needle (BD Insyte Autoguard Winged™, Becton Dickson Japan Co. Ltd., Fukushima, Japan) was placed in the ear vein of rabbit, through which was administered physiological saline by drip infusion at a rate of 60 mL/h. The anesthetic used was Nembutal™ (pentobarbital 50 mg/mL, Dainippon Pharmaceutical Co. Ltd., Osaka, Japan). Nembutal™ was diluted 10-fold in physiological saline and administered intravenously at an initial rate of 2 mL. Additional Nembutal™ was then appropriately administered by drip infusion at the rate of 1 mL each time such that the animal remained anesthetized without spontaneous respiration being suppressed.

The primary tumor, other tumors and lymph nodes were identified by normal B mode (basic ultrasound tomography) and recorded, and the size was measured.

The contrast agent Sonazoid™ is supplied as a lyophilized powder in vials and is reconstituted in 2 mL of distilled water prior to use. A total volume of 1 mL of Sonazoid™ was administered in aliquots of 0.25 mL to the subcutaneous tissues within the surroundings of the primary lesion or 5 mm of the tumor periphery in four locations (0, 3, 4, 6, and 9 o'clock). A 21G needle was used to make the subcutaneous injection. Then, a probe was placed in the direction of the long axis from the tumor or primary lesion of the hind paw towards the knee while massaging the tumor or tumor periphery. Imaging of the lymph duct was observed and a video recording and still images were recorded. In addition, a video recording and still images of the popliteal lymph node were observed and recorded.

The captured images were stored on the hard disk in the ultrasound device and the data was later extracted.

Histological examination

After the ultrasound observation, a total of 0.5 mL of blue dye (Patent Blue V sodium dye, Guerbert, Roissy, France) in aliquots of 0.125 mL was administered subcutaneously in almost the same four locations as the contrast agent. Then, the tumor or tumor periphery was massaged.

Fifteen minutes later, the rabbits were sacrificed by administering an overdose of Nembutal™ intravenously.

The skin of the legs was opened and subcutaneous tissue isolated. After confirming the blue stained lymph nodes, they were extracted. The extracted lymph nodes were fixed in 10% formaldehyde. Pathological specimen slides were then prepared. The specimens were stained with hematoxylin-eosin dye and observed microscopically.

The contrast-enhanced sonographic images and pathological tissue images that were obtained above were compared.

RESULTS

Contrast-enhanced ultrasonography of lymph ducts and lymph nodes

Sonazoid™ solution was injected subcutaneously and massage performed. Immediately after, both the tumor-induced and inflammation-induced enlargement models and the lymph ducts from the site of injection of the contrast agent in the hind paw to the popliteal lymph nodes were imaged (Figure 1). Imaging of the lymph ducts continued over several minutes. When imaging of the lymph ducts included the lymph node, the contrast agent entered the lymph nodes from the afferent duct and soon all the lymph nodes could be imaged. For some of the lymph nodes, the contrast agent leaked from the afferent duct (Figure 2).

Tumor-induced lymph node enlargement model

Models 1-6 are metastatic lymph node enlargement that was achieved by implanting VX2 tumor in hind paw of rabbits. Lymph node imaging was performed for all six animals that underwent contrast-enhanced sonography following implantation of the tumor. The period from the tumor transplant to the contrast-enhanced ultrasonography was 7-35 d. Enlarged popliteal lymph nodes with diameters of 12-18 mm were confirmed in the images taken by basic B mode (Figures 3A and 4A).

In model 1 (Table 1), only the periphery was enhanced. The central area was notably defective (Figure 3B). The histopathological images showed that most of the central area had changed into tumor while lymph tissue remained in the periphery (Figure 3C).

In model 2 (Table 1), only part of the periphery was enhanced and so most sites were not enhanced. The histopathological images showed that almost the entire area had changed into tumors while lymph tissue remained in only part of the periphery.

In models 3-5 (Table 1), a comparatively small defect was seen internally. The histopathological images showed that the site of that defect coincided with the site that had changed into tumor.

In model 6 (Table 1), the entire lymph nodes could

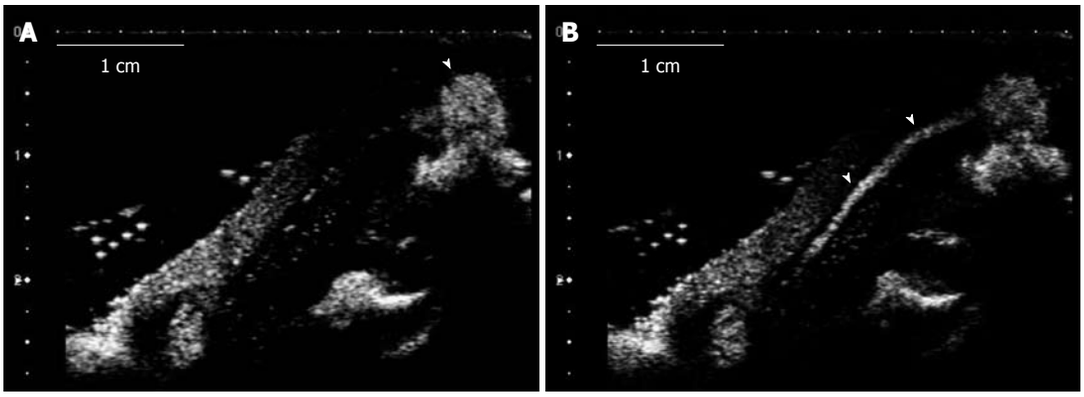

Figure 1 Ultrasound image of lymph ducts. Model of tumor-induced lymph node enlargement at 21 d after VX2 tumor was implemented (model 3). A: Sonazoid™ that was administered subcutaneously in the tumor lesion periphery of the hind paw. The arrowhead is the site where the contrast agent was injected; B: The lymph duct (arrowheads) towards the top part from the injection site that is shown in the form of a line.

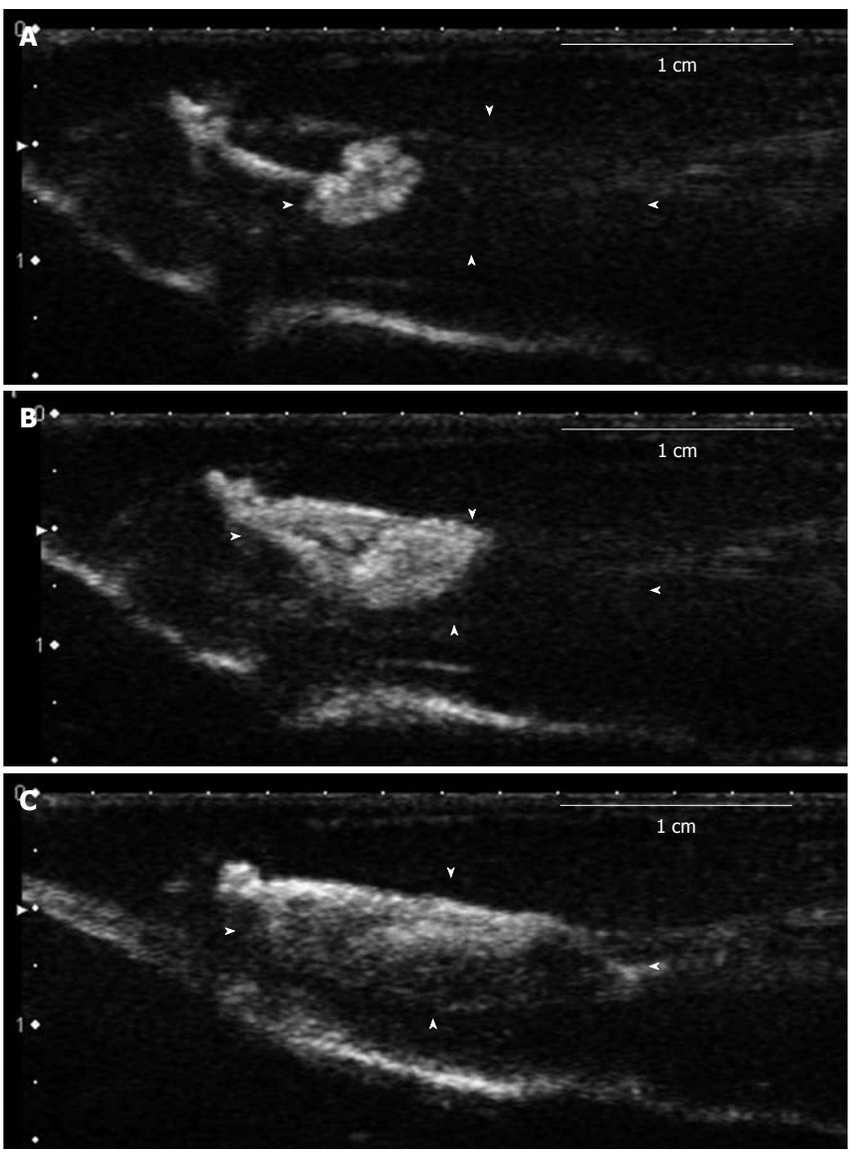

Figure 2 Lymph node imaging (dynamics study). The model of inflammation-induced lymph node enlargement at 3 d after *Escherichia coli* was implanted (model 8). A: The image of the lymph hilum 9 s later, showing flow of the contrast agent from the afferent lymph duct; B: The contrast agent reached the center of the lymph node from the lymph hilum 12 s later; C: The entire lymph node was imaged 15 s.

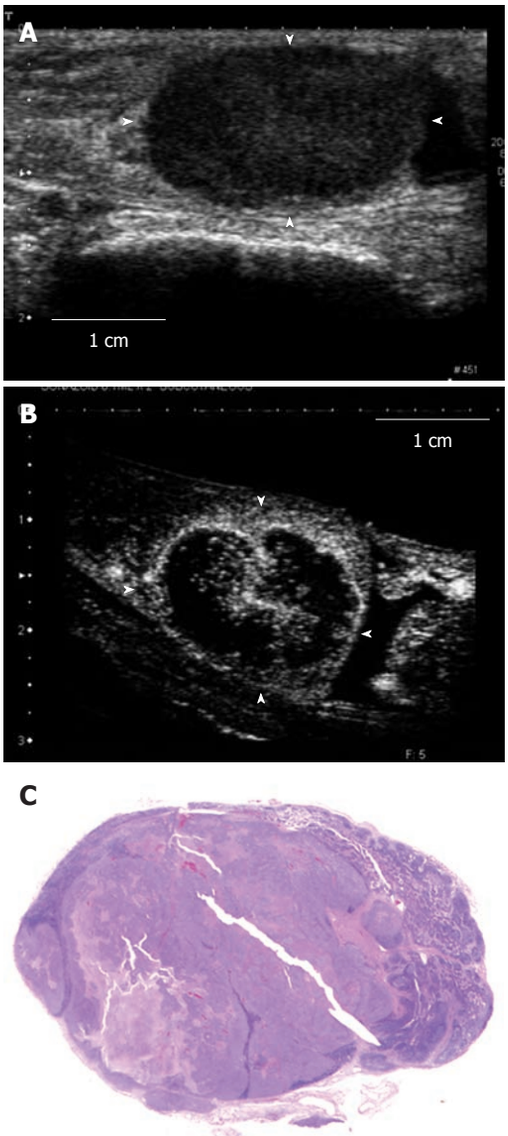

Figure 3 Contrast-enhanced ultrasonography image and histopathological image of the tumor-induced lymph node enlargement model. This is the tumor-induced lymph node enlargement model at 28 d after VX2 tumor was implanted (Model 1). A: The enlarged popliteal lymph node with a diameter of 18 mm that was seen in the B mode ultrasound image. This lymph node shown hypoechoic mass; B: Image of the popliteal lymph node that was imaged after the contrast agent was administered in the periphery of the primary tumor lesion. The central area is large and defective and so only the periphery of the lymph node was imaged; C: Histopathological image (hematoxylin-eosin stain) of the lymph node that was extracted. A large metastatic tumor lesion was seen in the center.

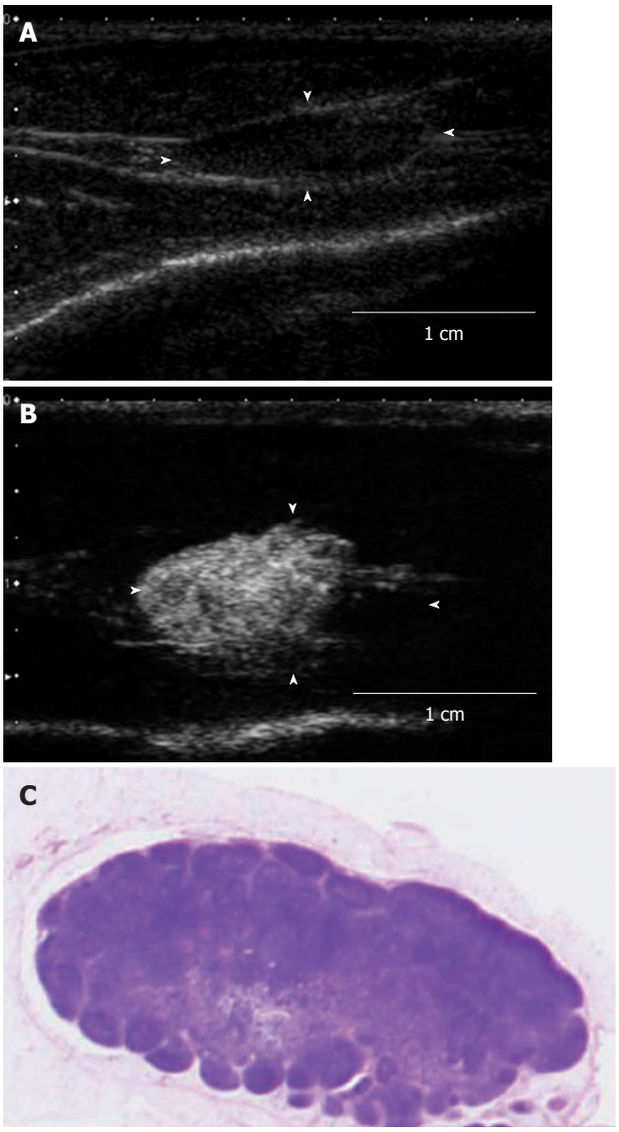

Figure 4 The contrast-enhanced ultrasonography image and histopathological image of the acute inflammation-induced lymph node enlargement model. The model of inflammation-induced lymph node enlargement at 7 d after *Escherichia coli* was implanted (model 9). A: The enlarged popliteal lymph node with a diameter of 13 mm that was seen in the B mode ultrasound image. This lymph node showed up as a hypoechoic mass; B: Image of the popliteal lymph node that was imaged after the contrast agent was administered in the periphery of the primary lesion. The entire lymph node was imaged; C: Histopathological image (hematoxylin-eosin stain) of the lymph node that was extracted. Invasion of inflammatory cells, mainly nucleocytes, was seen. These are findings of acute lymphadenitis.

be enhanced by contrast-enhanced ultrasonography. The histopathological images showed swollen inflammation-induced lymph nodes with no metastatic tumor lesions.

Inflammation-induced lymph node enlargement model

Models 7-11 (Table 1) are swollen inflammation-induced lymph nodes that were obtained by implanting *E. coli* into the hind paw of rabbits. The period from the infection to the contrast-enhanced ultrasonography was 3-18 d. Enlarged popliteal lymph nodes of diameter 8-17 mm were found during sonography. Images of these lymph nodes in basic B mode showed a flat condition compared to the VX2 tumor-induced metastasis model.

In models 8-10 (Table 1), contrast-enhanced ultrasonography showed that the entire lymph nodes were enhanced (Figure 4B). The contrast agent entered the lymph nodes from the afferent lymph duct. The lymph nodes were uniformly imaged gradually towards the trunk. Imaging of the efferent duct was minimal. The histopathological images showed strong infiltration of inflammatory cells, mainly of the mononuclear cells. In particular, follicular formation was seen in the central area. These were

Table 1 List of experimental models

Model No. #	Implanting	Days after implanting	Size of lymph node	Imaging findings in B mode	Imaging findings in contrast enhanced ultrasonography
1	VX2	28	18 × 11	Hypoechoic	Only the periphery was enhanced The central area was notably defective
2	VX2	28	18 × 10	Iso-hypoechoic	Only part of the periphery was enhanced. Most sites were not enhanced
3	VX2	21	15 × 10	Isoechoic	A comparatively small defect was seen internally
4	VX2	35	16 × 10	Hypoechoic	A comparatively small defect was seen internally
5	VX2	21	17 × 6	Hypoechoic	A comparatively small defect was seen internally
6	VX2	7	12 × 7	Iso-hypoechoic	The entire lymph node could be enhanced
7	*E. coli*	28	17 × 8	Iso-hypoechoic	The entire lymph node was enhanced (a defective star-like image was seen)
8	*E. coli*	3	8 × 3	Isoechoic	The entire lymph node was enhanced
9	*E. coli*	7	13 × 5	Iso-hypoechoic	The entire lymph node was enhanced
10	*E. coli*	3	9 × 3	Hypoechoic	The entire lymph node was enhanced
11	*E. coli*	3	8 × 3	Isoechoic	The entire lymph node was enhanced

The list of the tumor-induced and inflammation-induced lymph node enlargement models is shown. Models 1 to 6 are tumor-induced lymph node enlargement that was obtained by implanting VX2 tumor. Models 7 to 11 are inflammation-induced lymph node enlargement that was obtained by implanting *Escherichia coli* (*E. coli*).

findings of acute lymphadenitis (Figure 4C).

In models 7 and 11, the entire lymph nodes were enhanced non-uniformly by contrast-enhanced ultrasonography. In model 7, a defective star-like image was seen. In the histopathological image, inflammation-induced cell invasion and fiberization in the entire lymph nodes were seen while in model 11, there was lymph tissue in the periphery and inflammation-induced cell invasion as well as strong fiberization.

In sum, contrast-enhanced sonography of the tumor metastatic model revealed defective shadows in the lymph nodes. The one animal that had no defective part did not have tumor metastasis in the lymph nodes but was rather a case of enhanced inflammation (model 5). The contrast-enhanced ultrasonography of the five animals used for the inflammation-induced enlargement model showed that the short period that elapsed after staining contributed to the uniform staining trend while a long period resulted in non-uniform staining, which was consistent with the histopathological findings of chronic lymphadenitis with fiberization.

DISCUSSION

Contrast-enhanced ultrasonography was first reported by Gramiak in 1968[16]. Rapid intravenous injection of physiological saline enhanced the ultrasound signal in the right atrium[16]. The basic principle of contrast-enhanced ultrasonography lies on the separation of the ultrasound signals from tissues from ultrasound signals from the microbubbles. The ultrasound signal from organs is almost the same form as transmission pulses, whereas bubbles that have been bombarded with ultrasound waves behave in a complicated manner such as vibration, disappearance and fragmentation. The ultrasound signal released from the bubbles is of a different form compared to that of the transmission pulse, and is said to be a non-linear signal. Extraction of this non-linear signal is the basic principle of contrast-enhanced ultrasonography. To visualize information on microvascular flow that cannot be detected by power Doppler, a technique that is more effective at extracting the non-linear signal is necessary. Recent advances in devices have led to the appearance of non-linear imaging techniques such as second harmonic imaging and pulse inversion that are now being used clinically[11,17,18].

The active ingredient of Sonazoid™ is perflubutane (PFB) microbubble that was stabilized using hydrogenated egg phosphatidyl serine sodium (H-EPSNa), which is a phospholipid[19]. PFB is chemically stable and insoluble in water. Therefore, it has a long lifespan in the body because it hardly dissolves in the blood.

When the microbubble is bombarded with ultrasound waves with an acoustic pressure that is normally used clinically, it bursts easily. Sonazoid™ uses a single layer of H-EPSNa membrane, therefore it has superior ultrasound wave tolerance and has been designed such that non-linear ultrasound signals are produced consistently.

Sonazoid™ is classed as one of the second generation contrast agents. Compared to Definity™, it can be visualized at a comparatively high acoustic pressure. Therefore, it is classed as a moderate acoustic pressure contrast agent. It is comparatively hard, as fluorocarbon is enclosed in a shell and so has a comparatively long lifespan in the body.

The diameter of Sonazoid™ is 2-3 μm while the diameter of lymph ducts in subcutaneous tissue is normally 0.2-0.5 mm. Therefore, Sonazoid™ can easily move into lymph ducts. In addition, lymph ducts can be contrasted because hydrophobic bases are arranged on the membrane of the H-EPSNa shell and the shell is highly elastic.

Goldberg *et al*[13] extracted the sentinel lymph node following contrast-enhanced ultrasonography and observed it by electron microscopy. They confirmed the presence of spherical vacuoles in the cytoplasm of histiocytes (i.e. macrophages). The size of the vacuoles ranged from 1.07 to 1.99 μm. These vacuoles were not found anywhere else apart from the lymph node cells of the

histiocytes. In addition, they were not found in the histiocytes of the control lymph nodes. Therefore, it was concluded that the vacuoles that were seen in the histiocytes of the cytoplasm were the Sonazoid™ microbubbles that were phagocytosed. The fact that placing the Sonazoid™ microbubbles into lymph ducts is simple and that they are phagocytosed by macrophages in lymph nodes has led to the suggestion that the mechanism whereby the microbubbles are maintained is by their uptake by the sentinel lymph node. In addition, when Sonazoid™ is injected, it accumulates in reticuloendothelial organs such as the liver and spleen maintaining the actual contrast over long hours. This is called Kupffer imaging. The mechanism is suggested to be phagocytosis of the microbubbles by macrophages present in the endodermis of the liver and spleen[20].

Basically, lymphocytes, plasma cells and histiocytes make up the parenchyma and reticular fiber, blood vessels, lymphatic sinus endothelium, beam-columns and capsules make up the stroma. In addition, lymph nodes are modified according to the quality and quantity of immune stimulation they receive and individual responses, which are influenced by factors such as age and nutrition. Lymphocyte proliferation takes place in the lymph nodule aggregates present in lymphocytes. The filtering device used to process the lymphatic sinuses was bacterial and foreign body phagocytosis. Antibodies were produced. When foreign bodies such as pathogens enter lymph nodes, they become reddened and swollen in response resulting in increased weight[21].

Shope first reported that "Shope papilloma" is a tumor that proliferates in papilla that could be seen in cottontailed rabbits. It is caused by the virus *Parvoviridae* (Shope papilloma virus) and even when rabbits are infected with this virus, the same proliferation is induced. Of these tumors, the VX2 tumor, which has a high rate of malignancy is a successively transplanted stock that was established from epidermoid carcinoma[22,23].

Contrast-enhanced ultrasonography of the tumor metastatic model showed imaging and continued staining of the sentinel lymph nodes. Contrast-enhanced ultrasonography also revealed a region of defective shadows in that enlarged lymph node and was suggested to be the metastatic lesion. The minimum size of the lesion was 2-3 mm. Histological examination confirmed that the imaged area corresponded to the remaining lymph tissue while the area of the defective shadows was confirmed to be the metastatic lesion of the tumor.

In the inflammation-induced enlargement model, there was uniform staining but non-uniform imaging. Contrast imaging that was performed shortly after the infection showed comparatively uniform staining but the staining tended to be non-uniform in chronic-phase lymph nodes. Investigation of the histopathological images of the chronic lymph node enlargement model showed chronic lymphadenitis with fiberization. This was suggested not to be a reflection of non-uniform staining.

The above findings suggested that contrast-enhanced ultrasonography is useful in distinguishing tumor-induced and inflammation-induced lymph node enlargements. Omoto *et al*[11] reported a sentinel node detection method using contrast-enhanced ultrasonography with Sonazoid™ in a human breast cancer patient. The contrast-enhanced ultrasonography with Sonazoid™ for liver tumors has come to be generally performed in Japan[24,25]. The safety of Sonazoid™ in humans has been established. We want to continue with further study that compares tumor-induced and inflammation-induced lymph node enlargements using contrast-enhanced ultrasonography.

COMMENTS

Background

By using gaseous microbubbles, a strong contrast effect such as an echo source will be achieved. Sentinel node navigation surgery is becoming the focus of attention as a lowly invasive form of treatment for early cancer. Local injection of microbubble, which is a contrast agent, reveals the sentinel lymph node in ultrasonography

Research frontiers

A model of tumor-induced and a model of inflammation-induced swelling of lymph nodes were prepared to compare the differences between tumor-induced enlargement and inflammation-induced enlargement of lymph nodes using by contrast-enhanced ultrasonography.

Innovations and breakthroughs

Contrast-enhanced ultrasonography also revealed a region of defective shadows in the enlarged lymph node and this was suggested to be the metastatic lesion. In inflammation-induced swelling of lymph nodes models, contrast imaging that was performed shortly after the infection showed comparatively uniform staining but the staining tended to be non-uniform in chronic-phase lymph nodes.

Applications

Our study suggested that contrast-enhanced ultrasonography is useful in distinguishing tumor-induced and inflammation-induced lymph node enlargements.

Terminology

Sonazoid™ is a contrast agent that can be observed continuously with moderate acoustic pressure and without the microbubbles bursting.

Peer review

The paper can be accepted for publication in *World Journal of Radiology* after correction of many spelling and grammar mistakes.

REFERENCES

1 **Miller AP**, Nanda NC. Contrast echocardiography: new agents. *Ultrasound Med Biol* 2004; **30**: 425-434

2 **Morton DL**, Hoon DS, Cochran AJ, Turner RR, Essner R, Takeuchi H, Wanek LA, Glass E, Foshag LJ, Hsueh EC, Bilchik AJ, Elashoff D, Elashoff R. Lymphatic mapping and sentinel lymphadenectomy for early-stage melanoma: therapeutic utility and implications of nodal microanatomy and molecular staging for improving the accuracy of detection of nodal micrometastases. *Ann Surg* 2003; **238**: 538-549; discussion 549-550

3 **Albertini JJ**, Lyman GH, Cox C, Yeatman T, Balducci L, Ku N, Shivers S, Berman C, Wells K, Rapaport D, Shons A, Horton J, Greenberg H, Nicosia S, Clark R, Cantor A, Reintgen DS. Lymphatic mapping and sentinel node biopsy in the patient with breast cancer. *JAMA* 1996; **276**: 1818-1822

4 **Alazraki NP**, Styblo T, Grant SF, Cohen C, Larsen T, Aarsvold JN. Sentinel node staging of early breast cancer using lymphoscintigraphy and the intraoperative gamma-detecting probe. *Semin Nucl Med* 2000; **30**: 56-64

5 **Weisberg NK**, Bertagnolli MM, Becker DS. Combined sentinel lymphadenectomy and mohs micrographic surgery for high-risk cutaneous squamous cell carcinoma. *J Am Acad Dermatol* 2000; **43**: 483-488

6 **Zeitouni NC**, Cheney RT, Delacure MD. Lymphoscintigra-

phy, sentinel lymph node biopsy, and Mohs micrographic surgery in the treatment of Merkel cell carcinoma. *Dermatol Surg* 2000; **26**: 12-18
7 **Krag DN**, Weaver DL, Alex JC, Fairbank JT. Surgical resection and radiolocalization of the sentinel lymph node in breast cancer using a gamma probe. *Surg Oncol* 1993; **2**: 335-339; discussion 340
8 **Giuliano AE**, Kirgan DM, Guenther JM, Morton DL. Lymphatic mapping and sentinel lymphadenectomy for breast cancer. *Ann Surg* 1994; **220**: 391-398; discussion 398-401
9 **Koller M**, Barsuk D, Zippel D, Engelberg S, Ben-Ari G, Papa MZ. Sentinel lymph node involvement--a predictor for axillary node status with breast cancer--has the time come? *Eur J Surg Oncol* 1998; **24**: 166-168
10 **Giménez J**, Botella-Estrada R, Hernández D, Carbonell M, Martínez MA, Guillén C, Vázquez C. Anaphylaxis after peritumoral injection of sulphan blue 1% for identification of the sentinel node in lymphatic mapping of the breast. *Eur J Surg* 2001; **167**: 921-923
11 **Omoto K**, Matsunaga H, Take N, Hozumi Y, Takehara M, Omoto Y, Shiozawa M, Mizunuma H, Harashima H, Taniguchi N, Kawano M. Sentinel node detection method using contrast-enhanced ultrasonography with sonazoid in breast cancer: preliminary clinical study. *Ultrasound Med Biol* 2009; **35**: 1249-1256
12 **Goldberg BB**, Merton DA, Liu JB, Thakur M, Murphy GF, Needleman L, Tornes A, Forsberg F. Sentinel lymph nodes in a swine model with melanoma: contrast-enhanced lymphatic US. *Radiology* 2004; **230**: 727-734
13 **Goldberg BB**, Merton DA, Liu JB, Murphy G, Forsberg F. Contrast-enhanced sonographic imaging of lymphatic channels and sentinel lymph nodes. *J Ultrasound Med* 2005; **24**: 953-965
14 **Wang Y**, Cheng Z, Li J, Tang J. Gray-scale contrast-enhanced ultrasonography in detecting sentinel lymph nodes: an animal study. *Eur J Radiol* 2010; **74**: e55-e59
15 **Wang Y**, Wang W, Li J, Tang J. Gray-scale contrast-enhanced ultrasonography of sentinel lymph nodes in a metastatic breast cancer model. *Acad Radiol* 2009; **16**: 957-962
16 **Gramiak R**, Shah PM. Echocardiography of the aortic root. *Invest Radiol* 1968; **3**: 356-366
17 **Schrope B**, Newhouse VL, Uhlendorf V. Simulated capillary blood flow measurement using a nonlinear ultrasonic contrast agent. *Ultrason Imaging* 1992; **14**: 134-158
18 **Burns PN**, Wilson SR, Simpson DH. Pulse inversion imaging of liver blood flow: improved method for characterizing focal masses with microbubble contrast. *Invest Radiol* 2000; **35**: 58-71
19 **Sontum PC**. Physicochemical characteristics of Sonazoid, a new contrast agent for ultrasound imaging. *Ultrasound Med Biol* 2008; **34**: 824-833
20 **Yanagisawa K**, Moriyasu F, Miyahara T, Yuki M, Iijima H. Phagocytosis of ultrasound contrast agent microbubbles by Kupffer cells. *Ultrasound Med Biol* 2007; **33**: 318-325
21 **Kageyama K**. Reactions of the lymph node as an organ against various acute stimulations. *Acta Pathol Jpn* 1967; **17**: 240-251
22 **Rous P**, Beard JW. The progression to carcinoma of virus-induced rabbit papillomas (SHOPE). *J Exp Med* 1935; **62**: 523-548
23 **Bernat JA**, Ronfeldt HM, Calhoun KS, Arias I. Prevalence of traumatic events and peritraumatic predictors of posttraumatic stress symptoms in a nonclinical sample of college students. *J Trauma Stress* 1998; **11**: 645-664
24 **Numata K**, Luo W, Morimoto M, Kondo M, Kunishi Y, Sasaki T, Nozaki A, Tanaka K. Contrast enhanced ultrasound of hepatocellular carcinoma. *World J Radiol* 2010; **2**: 68-82
25 **Mita K**, Kim SR, Kudo M, Imoto S, Nakajima T, Ando K, Fukuda K, Matsuoka T, Maekawa Y, Hayashi Y. Diagnostic sensitivity of imaging modalities for hepatocellular carcinoma smaller than 2 cm. *World J Gastroenterol* 2010; **16**: 4187-4192

S- Editor Cheng JX **L- Editor** O'Neill M **E- Editor** Zheng XM